

On the Spin of the $X(3872)$

R. Faccini*, F. Piccinini[†], A. Pilloni* and A.D. Polosa*

**Dipartimento di Fisica and INFN, 'Sapienza' Università di Roma,*
Piazzale A. Moro 2, Roma, I-00185, Italy

[†]*INFN Pavia, Via A. Bassi 6, Pavia, I-27100, Italy*

Whether the much studied $X(3872)$ is an axial or tensor resonance makes an important difference for its interpretation. A recent paper by the BaBar collaboration [1] raised the viable hypothesis that it might be a $J^{PC} = 2^{-+}$ state based on the $\pi^+\pi^-\pi^0$ spectrum in the $X \rightarrow J/\psi \omega$ decays.

Starting from a general parametrization of the decay amplitudes for the axial and tensor quantum numbers of the X , we analyze two models that differ by the functional form used to define the decay momentum dependence of the strong couplings.

The level of agreement of the two models with data is interpreted with a statistical approach based on Monte Carlo simulations, to be robust against the dilution induced by the scarce sensitivity of the $X \rightarrow J/\psi \rho$ channel to the spin of the X . Such analysis returns a probability of 0.2% (0.7%) and 46% (11%) for the 1^{++} and 2^{-+} hypotheses respectively, for the two models used. Either way the preference for the $J^{PC} = 2^{-+}$ assignment is enhanced with respect to the original BaBar analysis calling for new data in the $\pi^+\pi^-\pi^0$ spectrum.

PACS: 13.25.Ft, 14.40.Rt

I. INTRODUCTION

Although the resonance $X(3872)$ is the most studied among the exotic XYZ states, since its discovery in 2003, its quantum numbers have not been definitively identified yet.

The CDF collaboration concluded from the analysis of the angular distributions and correlations of the X decay products that the possible quantum numbers are $J^{PC} = 1^{++}$ and 2^{-+} [2]. Similar results have been found very recently by the BELLE collaboration [3]. In the latter paper the $\pi^+\pi^-$ invariant mass distribution is analyzed under the 1^{++} and 2^{-+} hypotheses, finding preference for the former whereas no preferred assignment emerges if an interfering contribution with the isospin-violating decay $\omega \rightarrow \pi^+\pi^-$ is added to the amplitude.

The picture becomes more puzzling as one considers the analysis by the BaBar Collaboration of the decay $X \rightarrow \psi \pi^+\pi^-\pi^0$ [1]. The expected 3π invariant mass distribution agrees with data slightly better if the 2^{-+} signature is assumed. This result on the 3π spectrum was later confirmed in [4].

In a recent paper [5] the pion invariant masses in the decays $X \rightarrow \psi 2\pi$ and $X \rightarrow \psi 3\pi$ are simultaneously analyzed with a combined fit, concluding that present data favor the 1^{++} assignment. In our view the 2π channel is not able to resolve the two hypotheses despite the high statistics, and the way the fit was performed just leads to the dilution of the indications from the 3π channel.

In this paper we perform a fit to the same data with the following approach: *i*) we write the decay matrix elements for both the 1^{++} and 2^{-+} hypotheses as given by enforcing Lorentz and gauge invariance, *ii*) we give a functional dependency to the couplings on the decay momenta introducing a length scale R – which might be related to the finite size of the hadrons participating to the interactions, *iii*) we use the matrix elements of ρ and ω decays to take into account the appropriate decay waves. We do not pursue the Blatt-Weisskopf description as we find that all spin structure can appropriately be taken into account with no further approximations.

We perform a global fit to profit from the large sensitivity of the ρ channel to the decay radius and we adopt a statistical approach to estimate the confidence level of the two spin hypotheses that allows to exploit the larger sensitivity of the ω channel to the spin of the X state.

II. MATRIX ELEMENTS

The matrix elements describing the amplitudes $X \rightarrow \psi V$ (where $V = \rho, \omega$) are obtained by Lorentz, gauge invariance and parity considerations leading to the formulae reported below [4].

In the $X(1^{++})$ case we have

$$\langle \psi(\epsilon, p) V(\eta, q) | X(\lambda, P) \rangle = g_{1\psi V} \epsilon^{\mu\nu\rho\sigma} \lambda_\mu(P) \epsilon_\nu^*(p) \eta_\rho^*(q) P_\sigma \quad (1)$$

In the 2^{-+} case we have instead

$$\langle \psi(\epsilon, p) V(\eta, q) | X(\pi, P) \rangle = g_{2\psi V} T_A + g'_{2\psi V} T_B \quad (2)$$

where π is the polarization tensor for a spin two particle with mass¹ and a standard notation is used for the remaining polarization vectors. We find that T_A and T_B are given by

$$T_A = \epsilon^{*\alpha}(p) \pi_{\alpha\mu}(P) \epsilon^{\mu\nu\rho\sigma} p_\nu q_\rho \eta_\sigma^*(q) - \eta^{*\alpha}(q) \pi_{\alpha\mu}(P) \epsilon^{\mu\nu\rho\sigma} q_\nu p_\rho \epsilon_\sigma^*(p) \quad (4)$$

and

$$T_B = Q^\alpha \pi_{\alpha\mu}(P) \epsilon^{\mu\nu\rho\sigma} P_\nu \epsilon_\rho^*(p) \eta_\sigma^*(q) \quad (5)$$

where $Q = p - q$ and $P = p + q$.

In Refs. [1, 3, 5] the P -wave fit functions contain a Blatt-Weisskopf angular momentum barrier factor of the form $(1 + R^2 q^{*2})^{-1/2}$, where q^* is the X decay 3-momentum. The value of R cannot be extracted from data since the P -wave distribution will approach the S -wave distribution in the limit $R \rightarrow \infty$, so that if we let R free, the fit will not converge. On the other hand, in our discussion we do not need any barrier factor the decay wave being dictated by the expressions of the matrix elements. We instead take into account the finite size of the X (and of V and ψ as well) introducing a ‘polar’ form factor, namely

$$g \rightarrow \frac{g}{(1 + R^2 q^{*2})^n} \quad (6)$$

where g stands in general for $g_{1\psi V}$, $g_{2\psi V}$ and $g'_{2\psi V}$. We tested the values $n = 1$ and $n = 2$ (the latter coinciding with the Fourier transform of an exponential $g(r) \sim \exp(-r/R)$ strong charge distribution). Both fitting functions turn out to be rather effective in improving our results, with no significative change for the two choices of n . We also underscore that $g_{1\psi V}$ (regulating the S -wave decay) is assumed to have the same polar behaviour since Eq. (6) does not concern any orbital angular momentum considerations. The size parameters R_J will eventually be fitted from data.

As for the ρ and ω decay amplitudes, we use

$$\langle \pi^+(p) \pi^-(q) | \rho(\epsilon, P) \rangle = g_{\rho 2\pi} \epsilon \cdot p \quad (7)$$

which describes a P -wave decay (the square modulus of this matrix element is $g_{\rho 2\pi}^2$ times the decay momentum squared). For the ω we have

$$\langle \pi^+(p) \pi^-(q) \pi^0(r) | \omega(\epsilon, P) \rangle = g_{\omega 3\pi} \epsilon^{\mu\nu\rho\sigma} \epsilon_\mu p_\nu q_\rho r_\sigma \quad (8)$$

The last two couplings will simply be written in terms of the partial widths $\Gamma(\rho \rightarrow 2\pi)$ and $\Gamma(\omega \rightarrow 3\pi)$, as shown in the next section.

III. DECAY WIDTHS

We have to calculate the partial widths $\Gamma(X \rightarrow \psi \pi^+ \pi^-)$ and $\Gamma(X \rightarrow \psi \pi^+ \pi^- \pi^0)$. In what follows we will neglect the ρ - ω mixing which is left to consideration in Appendix A: actually we found that the introduction of the ρ - ω mixing goes in the direction of slightly improving the quality of our results. Yet, a couple of reasons to keep the analysis simpler at this stage, thus neglecting the ρ - ω mixing, are the following:

- The mixing was introduced in Ref. [6] as a free parameter to improve the quality of the fits in the 2π channel, in particular for the 2^- hypothesis. In our analysis we expect that the introduction of the mixing could produce a slight improvement of the fit only near 782 MeV (the pole of the ω); however, as we will show, our functions do fit very well the 2π data even without any mixing term.
- Roughly speaking, $R_{\text{mix}} \approx \sqrt{\Gamma_\omega \times \mathcal{BR}(\omega \rightarrow 2\pi) \times (\text{enhancement by phase space})} / \Gamma_\rho \approx 15\%$. Since the error on the fit parameters are of the same order, we might decide to neglect the mixing.

¹ The sum over polarizations is

$$\sum_{\text{pol}} \pi_{\mu\nu}(k) \pi_{\alpha\beta}^*(k) = \frac{1}{2} T_{\mu\alpha} T_{\nu\beta} + \frac{1}{2} T_{\mu\beta} T_{\nu\alpha} - \frac{1}{3} T_{\mu\nu} T_{\alpha\beta} \quad (3)$$

with $T_{\mu\nu} = -g_{\mu\nu} + k_\mu k_\nu / m^2$ and $k^2 = m^2$.

The partial widths in the narrow width approximation are [4]

$$\begin{aligned} \Gamma(X \rightarrow \psi \pi^+ \pi^-) &= \frac{1}{2J+1} \frac{1}{48\pi m_X^2} \int ds \sum_{\text{pol}} |\langle \psi \rho(s) | X \rangle|^2 p^*(m_X^2, m_\psi^2, s) \\ &\times \frac{1}{\pi} \frac{1}{(s - m_\rho^2)^2 + (m_\rho \Gamma_\rho)^2} \int d\Phi^{(2)} \sum_{\text{pol}} |\langle \pi^+ \pi^- | \rho(s) \rangle|^2 \end{aligned} \quad (9)$$

where by $d\Phi^{(2)}$ we mean the 2-body phase space measure. The decay momentum q^* in the matrix element $\langle \psi \rho(s) | X \rangle$ coincides with $q^* \equiv p^*(m_X^2, m_\psi^2, s)$; similarly for the width in $\psi \omega$ discussed below.

The sum over polarizations in (7), simply yields

$$\sum_{\text{pol}} |\langle \pi^+ \pi^- | \rho(s) \rangle|^2 = g_{\rho 2\pi} p^*(s, m_\pi^2, m_\pi^2)^2 \quad (10)$$

Finally, we can eliminate the coupling by evaluating the (10) on the mass-shell and by relating it to the partial width $\Gamma(\rho \rightarrow \pi\pi)$

$$g_{\rho 2\pi}^2 = 6m_\rho^2 \Gamma(\rho \rightarrow \pi\pi) \frac{4\pi}{p^*(m_\rho^2, m_\pi^2, m_\pi^2)^3} \quad (11)$$

Inserting the above expressions (10), (11) into (9) gives

$$\begin{aligned} \Gamma(X \rightarrow \psi \pi^+ \pi^-) &= \frac{1}{2J+1} \frac{1}{8\pi m_X^2} \int ds \sum_{\text{pol}} |\langle \psi \rho(s) | X \rangle|^2 p^*(m_X^2, m_\psi^2, s) \\ &\times \frac{1}{\pi} \frac{m_\rho \Gamma_\rho \mathcal{BR}(\rho \rightarrow \pi\pi)}{(s - m_\rho^2)^2 + (m_\rho \Gamma_\rho)^2} \frac{m_\rho}{\sqrt{s}} \left(\frac{p^*(s, m_\pi^2, m_\pi^2)}{p^*(m_\rho^2, m_\pi^2, m_\pi^2)} \right)^3 \end{aligned} \quad (12)$$

Similarly,

$$\begin{aligned} \Gamma(X \rightarrow \psi \pi^+ \pi^- \pi^0) &= \frac{1}{2J+1} \frac{1}{48\pi m_X^2} \int ds \sum_{\text{pol}} |\langle \psi \omega(s) | X \rangle|^2 p^*(m_X^2, m_\psi^2, s) \\ &\times \frac{1}{\pi} \frac{1}{(s - m_\omega^2)^2 + (m_\omega \Gamma_\omega)^2} \int d\Phi^{(3)} \sum_{\text{pol}} |\langle \pi^+ \pi^- \pi^0 | \omega(s) \rangle|^2 \end{aligned} \quad (13)$$

Summing over the ω polarizations one obtains

$$\sum_{\text{pol}} |\langle \pi^+ \pi^- \pi^0 | \omega(s) \rangle|^2 = \frac{g_{\omega 3\pi}^2 s}{s^3} \frac{1}{4} [(m_0^2 + s - 2\sqrt{s} \omega) (\omega^2 - m_0^2 - 4x^2) - 4m_+^2 (\omega^2 - m_0^2)] \equiv g_{\omega 3\pi}^2 \mathcal{M}(\sqrt{s}) \quad (14)$$

where $\omega = E_{\pi^0}$, $x = \frac{1}{2}(E_{\pi^+} - E_{\pi^-})$ and $m_0 = m_{\pi^0}$, $m_+ = m_{\pi^+} = m_{\pi^-}$. An adimensional coupling has been formed by substituting $g_{\omega 3\pi}^2 \rightarrow \frac{1}{s^3} g_{\omega 3\pi}^2$. We eliminate the coupling evaluating (14) on the mass-shell

$$g_{\omega 3\pi}^2 = 6m_\omega \Gamma(\omega \rightarrow 3\pi) \left(\int d\Phi^{(3)} \mathcal{M}(m_\omega) \right)^{-1} \quad (15)$$

Inserting (14), (15) into (13) we obtain:

$$\begin{aligned} \Gamma(X \rightarrow \psi \pi^+ \pi^- \pi^0) &= \frac{1}{2J+1} \frac{1}{8\pi m_X^2} \int ds \sum_{\text{pol}} |\langle \psi \omega(s) | X \rangle|^2 p^*(m_X^2, m_\psi^2, s) \\ &\times \frac{1}{\pi} \frac{m_\omega \Gamma_\omega \mathcal{BR}(\omega \rightarrow 3\pi)}{(s - m_\omega^2)^2 + (m_\omega \Gamma_\omega)^2} \frac{\Phi^{(3)'(\sqrt{s}, m_0, m_+, m_+)}}{\Phi^{(3)'(m_\omega, m_0, m_+, m_+)}} \end{aligned} \quad (16)$$

² This rescaling is arbitrary and in part relies on the narrowness of the ω . Avoiding the introduction of the $1/s^3$ term, the separate fit of 3π does not change significantly (for example, with $n = 1$, the 2^{-+} is unchanged, the 1^{++} gets worse from $\chi^2 = 9.9 \rightarrow 11.1$). In the combined fit both hypotheses become a bit worse (again for $n = 1$, 2^{-+} : $\chi^2 = 17.7 \rightarrow 18.4$; 1^{++} : $\chi^2 = 25.2 \rightarrow 26.2$) so that the $\Delta\chi^2$ remains almost unchanged. See Sec. V.

where

$$\Phi^{(3)'}(\sqrt{s}, m_0, m_+, m_+) = \frac{1}{32\pi^3} \int_{m_0}^{\omega_m} d\omega \int_{x_-}^{x_+} dx \frac{1}{4s^2} [(m_0^2 + s - 2\sqrt{s}\omega)(\omega^2 - m_0^2 - 4x^2) - 4m_+^2(\omega^2 - m_0^2)] \quad (17)$$

with $\omega_m = (m_0^2 - 4m_+^2 + s)/(2\sqrt{s})$ and

$$x_{\pm} = \pm \frac{1}{2} \sqrt{\frac{(\omega^2 - m_0^2)(\omega_m - \omega)\sqrt{s}}{4m_+^2 + (\omega_m - \omega)\sqrt{s}}} \quad (18)$$

to be compared to the notations used in [4].

As usual, in the calculations we use the so-called *comoving width*, i.e. we rescale the width in the denominators of (12) and (16) according to the standard prescription $m\Gamma \rightarrow (s/m)\Gamma$.

IV. THE COMBINED FIT

The two pions invariant mass spectrum is taken from a sample of $X \rightarrow \psi \pi^+ \pi^-$ events (Belle [3]) with an invariant mass in the interval $3.863 \text{ GeV} \leq m_{\psi 2\pi} \leq 3.881 \text{ GeV}$, while the three pions invariant mass spectrum is taken from BaBar [1], from a sample of $X \rightarrow \psi \pi^+ \pi^- \pi^0$ events with an invariant mass in the interval $3.8625 \text{ GeV} \leq m_{\psi 3\pi} \leq 3.8825 \text{ GeV}$.

Since the $m_{3\pi}$ spectrum extends beyond the region allowed for a on-shell X , we need to take into account the width of the X . Therefore we extract randomly the values of the mass of the X from a Breit-Wigner centered at $m_X = 3872 \text{ MeV}$ with $\Gamma_X = 1.7 \text{ MeV}$ [7], accepting only those values kinematically allowing the decay of interest. The resulting fits are shown in Fig. 1. The shape of the distributions at $m_{3\pi} = 775 \text{ MeV}$ is due to the end-point for the X being on-shell.

In the following we discuss separately the $n = 1$ and $n = 2$ cases of Eq. (6).

A. $n = 1$

First of all, we try to fit the 2π [3] and the 3π channels [1] separately, for both the spin hypotheses. We find that in the channel $X \rightarrow \psi 2\pi$, both hypotheses fit well the data.

1^{++} has a $\chi^2/\text{DOF} = 14.3/17$ (CL 64%), with a polar radius value of $R_1 = 1.7 \pm 0.3 \text{ GeV}^{-1}$; 2^{-+} has a $\chi^2/\text{DOF} = 15.1/16$ (CL 52%), with $R_2 = 6.5 \pm 1.4 \text{ GeV}^{-1}$.

For $X \rightarrow \psi 3\pi$, the 2^{-+} hypothesis has a $\chi^2/\text{DOF} = 1.5/3$ (CL 65%), with a polar radius value of $R_2 = 4.2 \pm 1.6 \text{ GeV}^{-1}$; on the contrary, the 1^{++} hypothesis fits poorly the spectrum: it has a $\chi^2/\text{DOF} = 9.9/4$ (CL 4%), with $R_1 = 0.0 \pm 1.6 \text{ GeV}^{-1}$.

It seems therefore that the 2π channel is not able to resolve between the hypotheses, while the 3π channel indicates $J^{PC} = 2^{-+}$ as the most likely one. This is consistent with the separate conclusions reached by Belle [3] and BaBar [1]. We want now to understand if a *combined* analysis of the two channels can help to improve the situation, in particular if we can exploit the copious 2π sample to constraint the radius and the more sensitive 3π sample to discriminate between the hypotheses.

The combined fit to test the 1^{++} hypothesis has three free parameters: the coupling constants $g_{1\psi\omega}$, $g_{1\psi\rho}$, and the radius of the polar form factor R_1 (the same scale is naturally taken for both $m_{2\pi}$ and $m_{3\pi}$ distributions).

On the other hand, the fit under the 2^{-+} hypothesis has five free parameters: $g_{2\psi\omega}$, $g'_{2\psi\omega}$ and $g_{2\psi\rho}$, $g'_{2\psi\rho}$, and the radius R_2 . We prefer to adopt the following parameterization

$$\begin{aligned} g_{2\psi\omega} &= r_{2\omega} \cos \frac{\theta_\omega}{2}, & g'_{2\psi\omega} &= r_{2\omega} \sin \frac{\theta_\omega}{2} \\ g_{2\psi\rho} &= r_{2\rho} \cos \frac{\theta_\rho}{2}, & g'_{2\psi\rho} &= r_{2\rho} \sin \frac{\theta_\rho}{2} \end{aligned} \quad (19)$$

We remark that the parameters r_{JV} do not have a direct physical meaning, because they actually are scale factors which can be calculated by imposing the correct overall normalization of $\Gamma(X \rightarrow \psi 2\pi, 3\pi)$. Performing the fit, we noted that the errors on $\theta_{\rho,\omega}$ are greater than 2π , i.e., the fit cannot resolve the composition of T_A and T_B into Eq. (2) due to their similar behavior as functions of s . We will therefore fix the two parameters to arbitrary values. Tab. I reports the numerical results of the fit.

It is interesting to note that the radii, which are the fit parameters with a physical content, have reasonably small errors and get values consistent with 1 fm, the scale of the size of a standard hadron.

	1^{++} (dashed curve)	2^{-+} (solid curve)
$r_{J\rho}$	0.089 ± 0.006 a.u.	0.7 ± 0.2 a.u.
$r_{J\omega}$	0.0026 ± 0.0003 a.u.	0.029 ± 0.016 a.u.
R_J	$1.6 \pm 0.3 \text{ GeV}^{-1}$	$5.6 \pm 0.8 \text{ GeV}^{-1}$
χ^2/DOF	25.2/22	17.7/20

TABLE I: The $n = 1$ case. Fitted values for couplings and $R_{J=1,2}$ for the two J^{PC} assignments. Here $r_{1V} = g_{1\psi V}$ and $V = \rho, \omega$. (a.u.=arbitrary units)

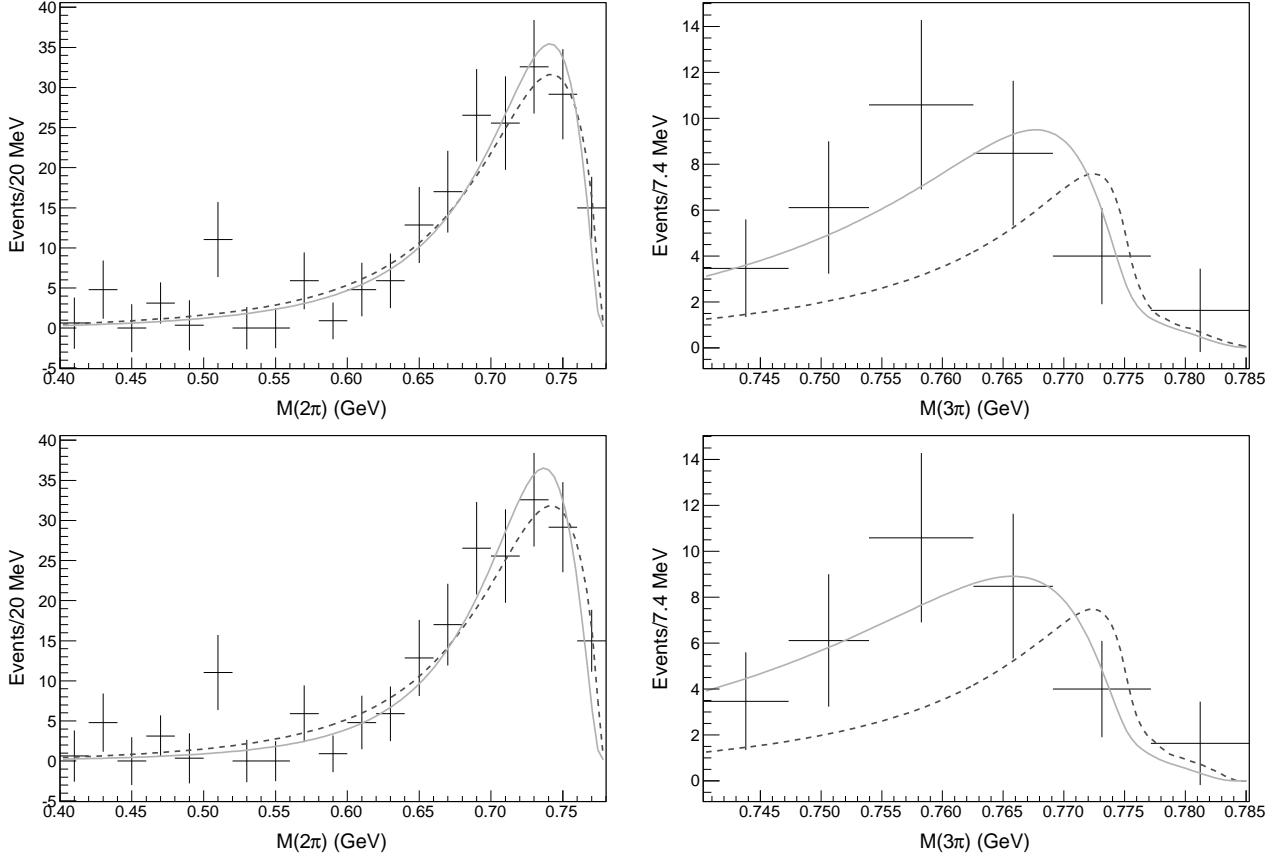


FIG. 1: Fit to the 2π (left) and 3π (right) samples as described in the text, with the model with $n = 1$. The dashed curve refers to the 1^{++} hypothesis, the solid one is for the 2^{-+} one. The top (bottom) rows correspond to $n = 1$ ($n = 2$).

B. $n = 2$

We report a few results for the form factor with $n = 2$. In general, the conclusions are the same as those discussed in the $n = 1$ case, with slightly smaller radii. For $X \rightarrow \psi 2\pi$, the 1^{++} hypothesis allows a fit with a $\chi^2/\text{DOF} = 14.0/17$ (CL 67%), with a polar radius value of $R_1 = 1.1 \pm 0.2 \text{ GeV}^{-1}$; on the other hand, the fit of 2^{-+} get slightly worse: $\chi^2/\text{DOF} = 17.2/16$ (CL 37%), with $R_2 = 2.8 \pm 0.3 \text{ GeV}^{-1}$. There is a slight preference for the 1^{++} , but certainly not enough to decide. For $X \rightarrow \psi 3\pi$, the χ^2 are almost the same as in the previous case. We only report that $R_1 = 0.0 \pm 1.1 \text{ GeV}^{-1}$, $R_2 = 2.7 \pm 0.9 \text{ GeV}^{-1}$.

As in the previous case, the fit cannot resolve the angles between the couplings of 2^{-+} . We therefore repeated the fits with some fixed values of θ , with not significative variations of χ^2 . Our conclusions are the same as in the previous case.

	1^{++} (dashed curve)	2^{-+} (solid curve)
$r_{J\rho}$	0.089 ± 0.006 a.u.	$\theta_\rho = \theta_\omega = 0 \rightarrow 0.56 \pm 0.07$ a.u. $\theta_\rho = \theta_\omega = \pi/2 \rightarrow 0.50 \pm 0.06$ a.u. $\theta_\rho = \theta_\omega = \pi \rightarrow 0.50 \pm 0.06$ a.u.
$r_{J\omega}$	0.0026 ± 0.0003 a.u.	$\theta_\rho = \theta_\omega = 0 \rightarrow 0.028 \pm 0.003$ a.u. $\theta_\rho = \theta_\omega = \pi/2 \rightarrow 0.024 \pm 0.003$ a.u. $\theta_\rho = \theta_\omega = \pi \rightarrow 0.024 \pm 0.003$ a.u.
R_J	1.1 ± 0.2 GeV $^{-1}$	2.8 ± 0.3 GeV $^{-1}$
χ^2/DOF	24.8/22	18.9/20

TABLE II: The $n = 2$ case. Fitted values for couplings and $R_{J=1,2}$ for the two J^{PC} assignments. (a.u.=arbitrary units). In this Table we also show explicitly the dependency on the θ fit parameters.

V. MEASUREMENT OF THE SPIN OF THE $X(3872)$

We examined the results of the combined fits described above with a statistical approach that allows to take into account the scarce sensitivity of the 2π channel to the spin hypotheses. On the basis of the χ^2 values returned by the fits, see Tabs. I and II, one would conclude that all the hypotheses are reasonably likely. In particular, for $n = 1$, the 1^{++} hypothesis with $\chi^2 = 25.2$ for 22 degrees of freedom has a probability of

$$P(\chi^2) = \int_{\chi^2}^{\infty} \text{PDF}(x, N_{\text{DOF}}) dx = 29\% \quad (20)$$

where $\text{PDF}(\chi^2, N_{\text{DOF}})$ is the probability density function of the χ^2 variable with N_{DOF} degrees of freedom. Such a large probability would indicate that the 1^{++} hypothesis fits the data well. Yet, the agreement between the 3π data and the model (right side of Fig. 1) seems worse than the quoted probability of 29%. Such a large probability of the combined fit is due to the good agreement between the more copious 2π data sample and the model (left side of Fig. 1). However the latter agreement is rather due to *lack of sensitivity* than to a true preference of the 2π channel for the 1^{++} hypothesis.

In support to this statement we performed a Monte Carlo (MC) study, that we next used to develop a sounder statistical approach. We generated N Monte Carlo data samples with the same number of events as the experimental samples and took into account the background, the statistical fluctuations, and the uncertainties in the model parameters. The simulations can be performed either by making the hypothesis that the X is truly a 1^{++} state or a 2^{-+} state.

As the starting point of the simulation for a given J and n hypothesis we take the corresponding model extracting sample by sample the parameters according to the result of the combined fit to the data. The MC samples are generated by filling the invariant mass bins b_i according to Poisson distributions with mean values μ_i corresponding, bin per bin, to the sum of the values expected from the model and the experimental background. After the Poisson extraction such background is subtracted. As errors on b_i we assume the statistical fluctuations on μ_i .

The N data samples obtained with this procedure are then analyzed with the same fitting function and statistical analysis as the experimental data. For each MC sample, we perform the combined fit with both J and n options: we get four χ^2 values for each sample.

In order to evaluate whether $P(\chi^2)$ introduced above is a good estimator of the likelihood of a given J, n hypothesis, Fig. 2 shows its distributions in the samples simulated with $J^{PC} = 2^{-+}, n = 1$ as truth.

This figure shows that due to the dilution of the 2π channel, the $P(\chi^2)$ variable is not too discriminant. Indeed, the $P(\chi^2) = 29\%$ obtained on data when performing the combined fit with the 1^{++} model is not inconsistent with the X being a 2^{-+} state, since there is a probability of 30% for this to happen.

A more robust method of testing the hypotheses is to choose as estimator the difference between the χ^2 obtained from the combined fits performed under the two J hypotheses [9]

$$\Delta\chi^2 = \chi^2(1^{++}) - \chi^2(2^{-+}) \quad (21)$$

Fig. 3 shows that the distribution of such variable is peaked around a negative value when the MC samples are generated with 1^{++} and, viceversa, it is peaked around a positive value when the samples are generated with 2^{-+} . These distributions are used to calculate the fraction of samples in which $\Delta\chi^2$ has a value larger

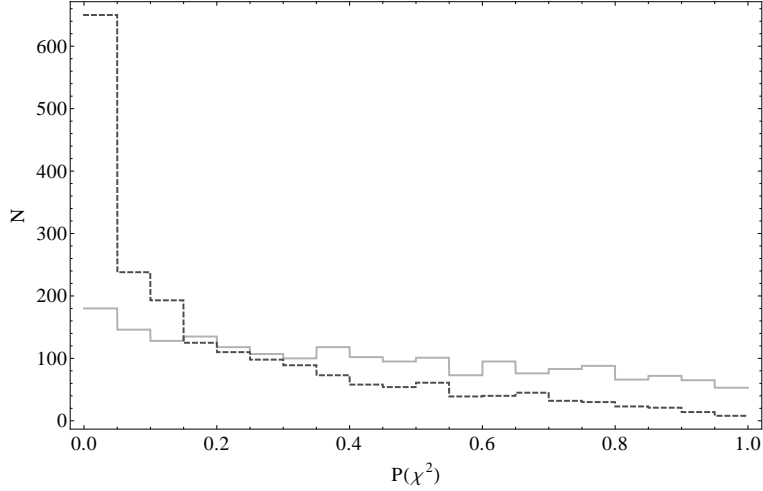


FIG. 2: Distribution of the $P(\chi^2)$ resulting from the combined fits to Monte Carlo data samples generated assuming 2^{-+} and $n = 1$. The solid (dashed) histogram corresponds to the fit to the 2^{-+} (1^{++}) and $n = 1$ model.

(for 1^{++}) or smaller (for 2^{-+}) than the one obtained on data. Such fraction estimates the probability of the hypothesis.

With this approach, in the case $n = 1$, where the fit to the data returns $\Delta\chi^2 = 7.5$ as shown in Tab. I, the probabilities for the two spin hypotheses are

$$\begin{aligned} P(\Delta\chi^2 > 7.5 | 1^{++}) &= 0.2\% \\ P(\Delta\chi^2 < 7.5 | 2^{-+}) &= 46\% \end{aligned} \quad (22)$$

The $J^{PC} = 1^{++}$ hypothesis is therefore highly disfavored, even more than in the original BaBar paper, due to the refinements made in the fitting technique and in the use of the 2π channel.

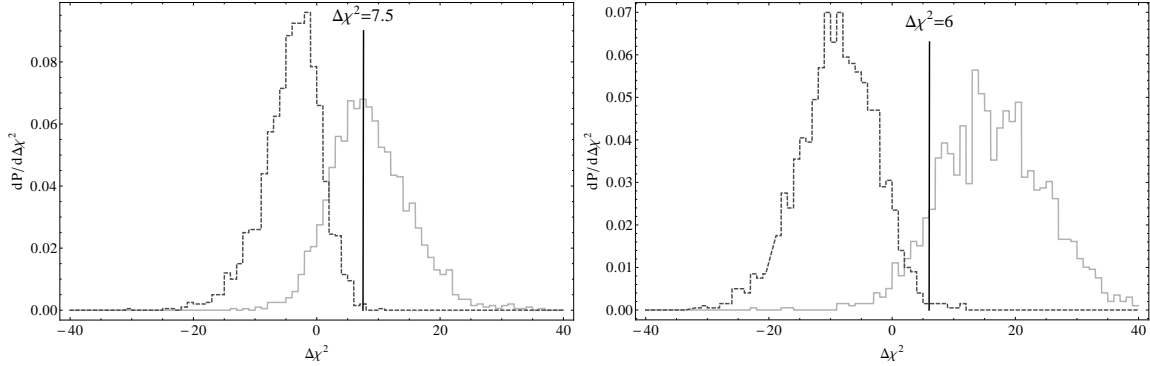


FIG. 3: Distribution of the $\Delta\chi^2$ resulting from the combined fits to Monte Carlo data samples with $n = 1$ (left) and $n = 2$ (right). The solid (dashed) histogram corresponds to events generated assuming the X to be a 2^{-+} (1^{++}) state. We mark with a line the position of the experimental $\Delta\chi^2$.

Similarly, in the case $n = 2$, where we obtain in data $\Delta\chi^2 = 6$ as shown in Tab. II, we calculate

$$\begin{aligned} P(\Delta\chi^2 > 6 | 1^{++}) &= 0.7\% \\ P(\Delta\chi^2 < 6 | 2^{-+}) &= 10.5\% \end{aligned} \quad (23)$$

Changing the form factor does not alter the conclusions, although the fit under the 2^{-+} hypothesis seems to prefer the $n = 1$ model.

VI. CONCLUSIONS

A fit to the $\pi^+\pi^-$ and $\pi^+\pi^-\pi^0$ invariant mass distributions in X to charmonium decays is performed in order to establish the spin of the X state. The X decay amplitudes are parameterized by some strong couplings, weighting terms written as products of momenta and polarizations as dictated by Lorentz, gauge and parity considerations. The strong couplings themselves are given a momentum dependency according to two models defined in Eq. (6) and identified by the $n = 1, 2$ parameter. These models require the introduction of an additional parameter R which can be related to the finite size of hadrons occurring in the interactions. The results, shown in Tab. I and II, are consistent with R of the order of the standard hadron size³.

In order to avoid biases we pursue a statistical approach based on Monte Carlo simulations of data samples. We tested whether the spin of the $X(3872)$ is $J^{PC} = 1^{++}$ or $J^{PC} = 2^{-+}$. A probability of 0.2% (0.7%) and 46% (11%) resulted for the 1^{++} and 2^{-+} hypotheses respectively, in the case $n = 1$ ($n = 2$). The preference for the $J^{PC} = 2^{-+}$ hypothesis for the X is thus enhanced with respect to what found in the original BaBar analysis due to the better model and to the use of the 2π channel to constrain the scale R .

Acknowledgements

We would like to thank F.C. Porter for the discussion on the statistical approach, and F. Renga for the analysis of experimental data about the width of the X . We also wish to thank C. Sabelli for her collaboration in the early stages of this work.

Appendix A: ρ - ω mixing

As discussed in Sec. III, the isosping-violating ρ - ω mixing introduces a correction near the pole of the ω , without affecting the core of our analysis. Moreover, we found that the mixing improves the quality of the fit of 2^{-+} and worsens the 1^{++} , so that our conclusions would be strengthened.

First of all, we have to insert the mixing into (9) and (13). Following Ref. [5], we describe the decay $\omega \rightarrow 2\pi$, as the oscillation $\omega \rightarrow \rho \rightarrow 2\pi$, as explained in Fig. 4. We call $-\epsilon$ the coupling of the vertex $\rho\omega$, whose value can be extracted by [5, 11]:

$$\epsilon \approx \sqrt{m_\omega m_\rho \Gamma_\rho \Gamma_\omega \mathcal{BR}(\omega \rightarrow 2\pi)} \approx 3.4 \cdot 10^{-3} \text{ GeV}^2 \quad (\text{A1})$$

The choice to treat the mixing reproduces naturally the phase of 95° of the complex mixing parameter used in Ref. [3].

Under the hypothesis 1^{++} we have

$$\langle \psi \rho(q) | X \rangle = g_{1\psi\rho} T - \epsilon g_{1\psi\omega} \frac{1}{q^2 - m_\omega^2 + im_\omega \Gamma_\omega} T \quad (\text{A2})$$

where T is the S-wave tensor described in (1). Similarly for 2^{-+}

$$\langle \psi \rho(q) | X \rangle = (g_{2\psi\rho} T_A + g'_{2\psi\rho} T_B) - \epsilon \frac{g_{2\psi\omega} T_A + g'_{2\psi\omega} T_B}{q^2 - m_\omega^2 + im_\omega \Gamma_\omega} \quad (\text{A3})$$

We can repeat the same argument for $\langle \psi \omega(q) | X \rangle$ by swapping the role of ρ and ω . The rest of Eqs. (12) and (16) (namely the Breit-Wigner and the decay into pions) stays unchanged, because in this picture it is only the ρ (resp. the ω) which can decay in 2π (3π), being the mixing exhausted in the $\langle \psi V | X \rangle$ matrix.

Moreover, if we take the mixing into account, the parameters $r_{J\rho}$ and $r_{J\omega}$ of the fit appear together in both channels; therefore we must impose their correct relative normalization. This can be solved by imposing that $\Gamma(X \rightarrow \psi 3\pi) / \Gamma(X \rightarrow \psi 2\pi) = 0.8 \pm 0.3$ [1, 7].

We can now perform again the fit of Eqs. (12) and (16) in the case $n = 1$, including the ρ - ω mixing. The hypothesis 1^{++} gets even worse, with a $\chi^2/\text{DOF} = 29/22$ (CL 15%), whereas the goodness of the 2^{-+} hypothesis is slightly improved, with a $\chi^2/\text{DOF} = 16/20$ (CL 71%).

³ Loosely bound molecules [8] are expected to be large size objects, as large as ~ 10 fm [10]

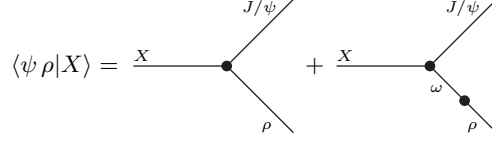


FIG. 4: Feynman diagrams of $X \rightarrow \psi \rho$ including the ρ - ω mixing. The second diagram includes the coupling ϵ and the propagator of the ω .

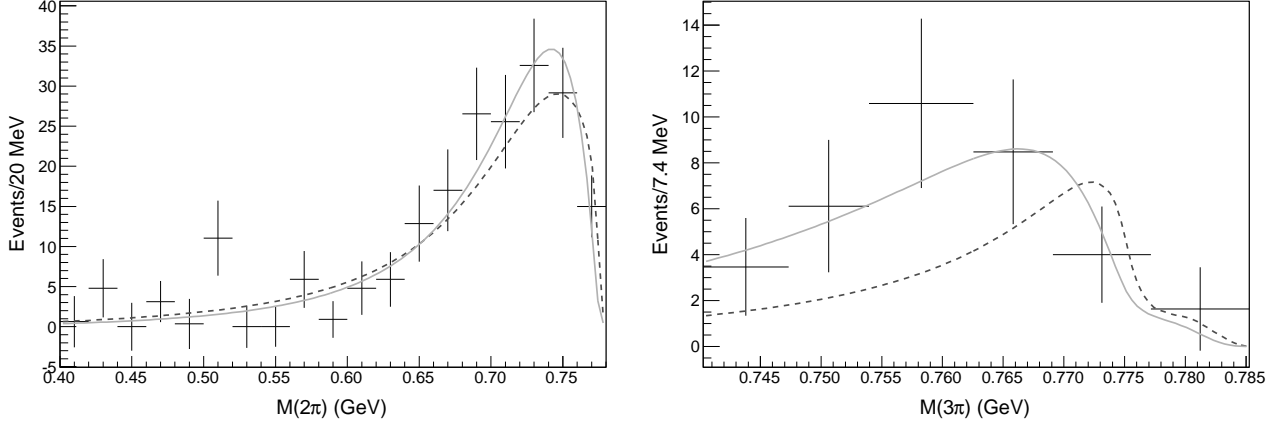


FIG. 5: Fit including ρ - ω mixing to the 2π (left) and 3π (right) samples, with the model with $n = 1$. The dashed curve refers to the 1^{++} hypothesis, the solid one is for the 2^{-+} one.

One could have thought that the presence of the narrow propagator of the ω would have constrained the fit to create a peak at $m_\omega = 782$ MeV. The smallness of ϵ , instead, does not allow this behavior, and the curve stays smooth at the pole, coherently with Refs. [3, 5, 6].

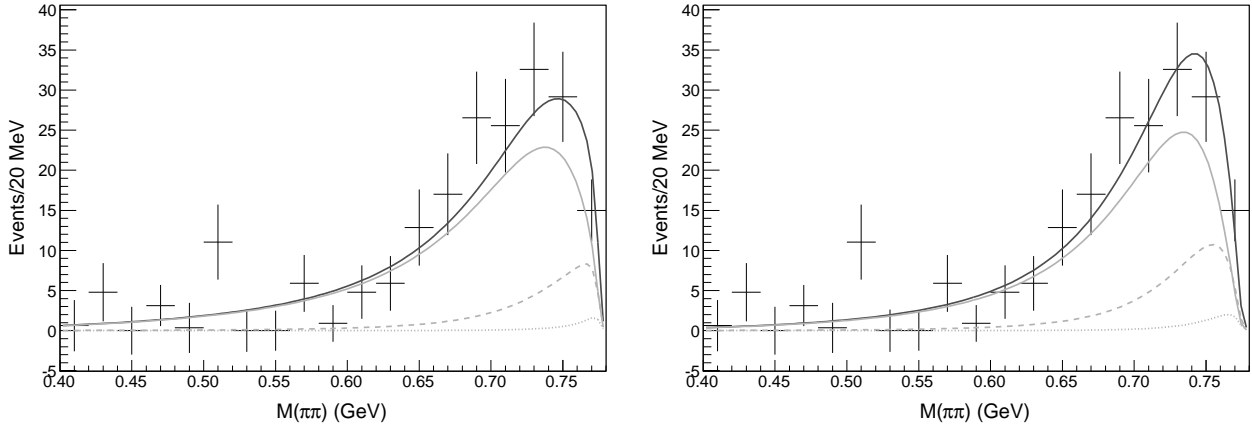


FIG. 6: 2π channel of the combined fit including ρ - ω mixing, with the model with $n = 1$, and with the signatures 1^{++} (left) and 2^{-+} (right). the solid light curve is the ρ contribution to the fit; the dotted light curve is the ω contribution, and the dashed curve is the interference term. The dark curve is the sum of all contributions.

- [1] P. del Amo Sanchez *et al.* [BABAR Collaboration], Phys. Rev. D **82** (2010) 011101 [arXiv:1005.5190 [hep-ex]].
 [2] A. Abulencia *et al.* [CDF Collaboration], Phys. Rev. Lett. **98** (2007) 132002 [arXiv:hep-ex/0612053].

- [3] S. -K. Choi, S. L. Olsen, K. Trabelsi, I. Adachi, H. Aihara, K. Arinstein, D. M. Asner and T. Aushev *et al.*, Phys. Rev. D **84** (2011) 052004 [[arXiv:1107.0163](#) [[hep-ex](#)]].
- [4] F. Brazzi, B. Grinstein, F. Piccinini, A. D. Polosa and C. Sabelli, Phys. Rev. D **84** (2011) 014003 [[arXiv:1103.3155](#) [[hep-ph](#)]].
- [5] C. Hanhart, Y. S. Kalashnikova, A. E. Kudryavtsev and A. V. Nefediev, Phys. Rev. D **85** (2012) 011501 [[arXiv:1111.6241](#) [[hep-ph](#)]].
- [6] A. Abulencia *et al.* [CDF Collaboration], Phys. Rev. Lett. **96** (2006) 102002 [[arXiv:hep-ex/0512074](#)]. [[hep-ex/0512074](#)].
- [7] N. Drenska, R. Faccini, F. Piccinini, A.D. Polosa, F. Renga and C. Sabelli, Riv. Nuovo Cim. **033**, 633 (2010) [[arXiv:1006.2741](#) [[hep-ph](#)]].
- [8] E. Braaten and M. Kusunoki, Phys. Rev. D **69**, 074005 (2004) [[arXiv:hep-ph/0311147](#)]. S. Pakvasa and M. Suzuki, Phys. Lett. B **579**, 67 (2004) [[arXiv:hep-ph/0309294](#)]. M. B. Voloshin, Phys. Lett. B **579**, 316 (2004) [[arXiv:hep-ph/0309307](#)]. M. B. Voloshin, Phys. Lett. B **604**, 69 (2004) [[arXiv:hep-ph/0408321](#)].
- [9] L. Demortier, “P values and nuisance parameters”, into L. Lyons, (ed.), H. B. Prosper, (ed.) and A. De Roeck, (ed.), “Statistical issues for LHC physics. Proceedings, Workshop, PHYSTAT-LHC, Geneva, Switzerland, June 27-29, 2007”, [<http://phystat-lhc.web.cern.ch/phystat-lhc/proceedings.html>]
- [10] C. Bignamini, B. Grinstein, F. Piccinini, A. D. Polosa and C. Sabelli, Phys. Rev. Lett. **103**, 162001 (2009) [[arXiv:0906.0882](#) [[hep-ph](#)]].
- [11] H. B. O’Connell, B. C. Pearce, A. W. Thomas and A. G. Williams, Prog. Part. Nucl. Phys. **39** (1997) 201 [[arXiv:hep-ph/9501251](#)].